BOREAL ENVIRONMENT RESEARCH 12: 265–278 ISSN 1239-6095
Helsinki 25 June 2007

The ^{222}Rn activity concentration, external radiation dose and air ion production rates in a boreal forest in Finland between March 2000 and June 2006

Anne Hirsikko[1)], Jussi Paatero[2)], Juha Hatakka[2)] and Markku Kulmala[1)]

[1)] *Department of Physical Sciences, P.O. Box 64, FI-00014 University of Helsinki, Finland*
[2)] *Finnish Meteorological Institute, P.O. Box 503, FI-00101 Helsinki, Finland*

Received 27 Oct. 2006, accepted 19 Dec. 2006 (Editor in charge of this article: Veli-Matti Kerminen)

Hirsikko, A., Paatero, J., Hatakka, J. & Kulmala, M. 2007: The ^{222}Rn activity concentration, external radiation dose and air ion production rates in a boreal forest in Finland between March 2000 and June 2006. *Boreal Env. Res.* 12: 265–278.

We measured the ^{222}Rn content of the air by continuously collecting particle-bound daughter nuclides ^{214}Pb and ^{214}Bi onto glass-fibre filters and counting their beta particle emissions with Geiger-Müller tubes. A scintillation gamma spectrometer system measured external radiation, which main components are gamma and cosmic radiation. Our purpose was to detect long-term, seasonal and diurnal variations in ^{222}Rn activity concentration and external radiation dose rate in a Finnish boreal forest during the years 2000–2006. The long-term variations in activity concentration and dose rate were small, whereas the annual variations were more pronounced. In late summer and autumn, the diurnal cycle of ^{222}Rn activity concentration was strongest, whereas the diurnal cycle of external radiation dose rate was practically non-existing throughout the year. We utilised the ^{222}Rn and external radiation measurements also when calculating air ion production rate in the lower boundary layer. Based on our results, the total ion production rate varied in the range 4.2–17.6 ion pairs cm^{-3} s^{-1}. The fraction of ^{222}Rn contribution in the ion production varied in the range 0–0.43, with average fraction 0.11 ± 0.07. These results indicate that ion production was typically dominated by the external radiation on our measurement site.

Introduction

Air ions are produced mainly by airborne radionuclides and external radiation in fair weather conditions. The latter has two main components, the cosmic radiation and gamma radiation from the ground. Cosmic radiation has a significant contribution to the total ionisation rate in the ground-level air and its importance increases with the increasing elevation. Gamma radiation from the ground originates from natural radioactivity, e.g. uranium and its decay series, and primordial radionuclides like potassium-40, incorporated in the Earth's crust. A small part of the gamma radiation comes from the natural and artificial radionuclides deposited on the ground or suspended in the air. The dose rate in the ground-level air caused by the external radiation varies in Finland between 0.04 and 0.3 μGy h^{-1} (1 Gy = 1 J kg^{-1}), the minimum value being due to the cosmic radiation (Mustonen 2006).

The most prominent natural radionuclide in surface air is radon-222 (^{222}Rn, $t_{1/2}$ = 3.825 d). It is produced in the soil from the decaying radium-

226 as a part of the natural decay series starting from uranium-238. In addition to isotope 222, ^{220}Rn from the thorium-232 series can be found in the atmosphere. Part of the radon produced in the surface soil can escape to the atmosphere because it is a noble gas. Radon-222 decays via several short-lived daughter nuclides to the relatively long-lived lead-210. Radon can be used as a tracer for continental air masses because its emission rate from oceans is negligible as compared with that from land areas (Baskaran *et al*. 1993). In Finland, as in a number of other countries, indoor radon is the most significant source of radiation exposure of the general public. Gesell (1983) and Porstendörfer (1994) reviewed studies on radon in indoor and outdoor air.

In the air, ^{222}Rn appears as single gas atoms, whereas its progeny are heavy metal atoms and are attached to airborne aerosol particles within 1 to 100 seconds. Most of the ^{222}Rn progeny are to be found in accumulation-mode aerosol particles with an aerodynamic diameter of a few hundred nanometres (Porstendörfer 1994, Porstendörfer and Reineking 1999). In Finland, the average ^{222}Rn activity concentration in the ground-level air is usually about 1 Bq m^{-3} (1 Bq = 1 disintegration per second) but large variations occur (Mattsson 1970).

The process, in which high energetic radiation ionises air molecules to positive ion and electron pairs (Israël 1970), is called ion production. In practise the total ion production rate in the air is governed by the external radiation and ^{222}Rn. As compared with them, the other sources of ionisation, e.g. airborne artificial and cosmogenic nuclides, are negligible. The new ions react with other air molecules and form cluster ions, which are observed to exist all the time in various environments (e.g. Hõrrak *et al*. 2003, Hirsikko *et al*. 2005), and they typically are the source of the electric charge of larger aerosol particles (Israël 1970). Cluster ions either attach on aerosol particle or other surfaces, recombine with a cluster of opposite polarity or act as intermediate in particle formation. Such a particle formation process is called ion-induced nucleation, which is either ion mediated heterogeneous nucleation or ion cluster activation. The ion-induced nucleation could participate in particle formation process in the atmosphere (e.g. Laakso *et al*. 2007). Although, many different mechanisms are proposed to produce aerosol particles (Kulmala 2003), the exact contribution of different formation mechanisms is somewhat unclear at the moment.

The ion-induced nucleation is limited by the ion production rate (e.g. Israël 1970). Therefore, it is important to know the daily, annual and long-term behaviours of ion production rate when aiming to estimate the importance of ion-induced nucleation as compared with particle formation by neutral mechanisms. Laakso *et al*. (2004) and Tammet *et al*. (2006) measured or estimated the ion production only for short periods (max. one month) at the Hyytiälä measurement station, Finland (Hari and Kulmala 2005), where we have one of the world's longest aerosol particle size distribution dataset for particle formation study (Dal Maso *et al*. 2005).

In this paper, we introduce our ^{222}Rn and external radiation measurements at the Hyytiälä measurement station. Strictly speaking we measured the equilibrium-equivalent decay product concentration of ^{222}Rn because the measurement was based on the collection and counting of the short-lived radon progeny nuclides assumed to be in equilibrium with ^{222}Rn. However, for brevity we use the term ^{222}Rn activity concentration in the following. We utilised the results of six-year and three-month measurements (March 2000–June 2006) to present ^{222}Rn activity concentrations and external radiation dose rates. From these results we calculated the ion production rate at our measurement site to obtain long-term information about the diurnal and seasonal variations of this important quantity.

Measurements and methods

We measured both the ^{222}Rn content of the air and external radiation at the Hyytiälä forestry field station of the University of Helsinki (61°51´N, 24°17´E, 180 m above sea level) in southern Finland. The station is located on a hill and the ground slopes downwards on every direction. The slope is the steepest towards the south and west and gentlest towards the north. Furthermore, the station is inside a large conifer-

ous forest dominated by Scots pine (*Pinus sylvestris*). The soil is haplic podzol and the parent material is coarse silty glacial till. Kulmala *et al.* (2001b), and Hari and Kulmala (2005) described the station and its operation in details.

We conducted the ^{222}Rn and external radiation measurements at 6 m and 1.5 m heights, respectively. The obtained results for the ^{222}Rn activity concentration represent only the measurement height since radon activity concentration depends on the height. Firstly, the ground is the source of radon gas. Secondly, the mixing conditions of the atmosphere have a strong effect on the activity concentration as a function of height. On the contrary, the external radiation measurements represent the conditions of several tens of meters due to the small variation as a function of height. The external radiation dose rate is mainly due to the gamma radiation from the ground and cosmic radiation.

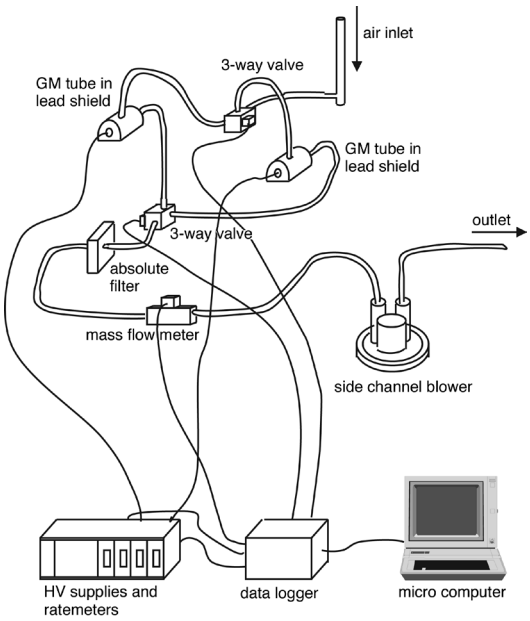

Fig. 1. Experimental setup for ^{222}Rn measurements at Hyytiälä.

Measurements of ^{222}Rn

Radon-222 is a noble gas and thus cannot be collected with aerosol filters. Therefore we measured its concentration via its short-lived daughter nuclides ^{214}Pb and ^{214}Bi which are bound to aerosol particles (Paatero *et al.* 1994). We monitored the concentration of these beta emitters with a system where air is drawn alternately through two cylindrical filters in four-hour periods (Fig. 1). Two cylindrical Geiger-Müller (GM) counters mounted co-axially inside the filters continuously recorded the beta activity accumulating onto the filters. The filters, with the GM tubes, were located inside lead shields to reduce the background count rates. The filter material was glass-fibre (Whatman GF/A), and we changed the filters every second Monday. The air flow rate was ca. 20 m^3 h^{-1}, which was measured with a mass flow meter that was protected by an absolute filter. The data logger counted the pulses from the GM tubes, and the count results were fed into the computer at 10-minute intervals for further analysis. The number of collected counts per interval usually varied from 300 to several thousands.

The method to distinguish the beta activity of the short-lived ^{222}Rn progeny from the ^{220}Rn progeny and artificial radioactivity is based on half-life differences. When the air begins flowing through a filter, the count rate of the corresponding GM tube increases from the base line as beta activity gathers onto the filter (collection period). After four hours the data logger switches the air flow to the second filter with the magnetic 3-way valves. The count rate of the first GM tube begins decreasing as the activity on the filter decays (decay period). If the activity is due to ^{222}Rn progeny only, the count rate returns to the base line during the decay period. However, if some long-lived activity such as ^{220}Rn progeny or artificial activity is present, the count rate remains at a higher level after the decay period.

The short-lived ^{222}Rn progeny consists of four nuclides: ^{218}Po ($t_{1/2}$ = 3.05 min), ^{214}Pb ($t_{1/2}$ = 26.8 min), ^{214}Bi ($t_{1/2}$ = 19.8 min) and ^{214}Po ($t_{1/2}$ = 162 μs). The activity of ^{214}Po, which has a short half-live, is equal to its predecessor ^{214}Bi. However, the Po isotopes are alpha emitters and do not contribute to the GM tube count rate. The activity concentration of ^{218}Po in the air is almost the same as the activity concentration of ^{222}Rn and can be calculated from the measured count rates by making two assumptions. Firstly, the measured beta activity originates only from

the short-lived beta emitters of ^{222}Rn progeny. Secondly, the activity concentration ratio among ^{218}Po, ^{214}Pb, and ^{214}Bi is constant and known. Here we assumed that the activity concentrations of the three nuclides are equal. The detector counting efficiencies for beta particles of ^{214}Pb and ^{214}Bi were 0.96% and 4.3%, respectively, in our counting geometry. During the collection period the activity concentration A can be calculated from the equation:

$$A = \frac{R}{V\varepsilon_2\left(\frac{S_1}{\lambda_1}+\frac{S_2}{\lambda_2}\right)+V\varepsilon_3\left(\frac{S_3}{\lambda_1}+\frac{S_4}{\lambda_2}+\frac{S_5}{\lambda_3}\right)} \quad (1)$$

where R is the count rate difference between two successive 10-minute intervals corrected for the decay of ^{214}Pb and ^{214}Bi already present on the filter. The subscripts 1, 2 and 3 refer to ^{218}Po, ^{214}Pb and ^{214}Bi, respectively. V is the flow rate of the air, ε the counting efficiency and λ the decay constant. The terms S_i are:

$$\begin{aligned}
S_1 &= 1 - Q_{2,1}e^{-\lambda_1 t}Q_{1,2}{}^{-\lambda_2 t}\\
S_2 &= 1 - e^{-\lambda_2 t}\\
S_3 &= 1 - Q_{2,1}Q_{3,1}e^{-\lambda_1 t} - Q_{1,2}Q_{3,2}e^{-\lambda_2 t} - Q_{1,3}Q_{2,3}e^{-\lambda_3 t} \quad (2)\\
S_4 &= 1 - Q_{3,2}e^{-\lambda_2 t} - Q_{2,3}e^{-\lambda_3 t}\\
S_5 &= 1 - e^{-\lambda_3 t}
\end{aligned}$$

where $Q_{i,j}$ is an abbreviation for $\lambda_i/(\lambda_i - \lambda_j)$. The S_i terms are constants if the time interval t in the measurements is constant, as we had.

The calculations of ^{218}Po ($\approx$ ^{222}Rn) activity concentrations are based on these equations after subtraction of baseline values from the measured gross count rates. The baseline count rate is due to the instrumental background and long-lived activity present on the filter. We assumed the long-lived activity concentration in the air to be constant during the collection period. The baseline is interpolated from the count rates at the end of the decay period and the count rate at the end of the previous decay period eight hours earlier. We calculated the activity concentration of ^{222}Rn in 10-minute intervals and then averaged the results over one hour. The counting error varies broadly depending mainly on the ^{222}Rn activity concentration but is usually of the order of 10%.

We calculated the ion-pair production rate (ion pairs cm^{-3} s^{-1}) caused by ^{222}Rn and its short-lived progeny by taking into account the total energy of the three alpha particles (^{222}Rn, ^{218}Po, and ^{214}Po) and two beta particles (^{214}Pb and ^{214}Bi) and by assuming that on average 34 eV (5.4×10^{-18} J) is needed to produce an ion pair in the air. The average beta particle energy of both ^{214}Pb and ^{214}Bi was used. We omitted the energy of the simultaneous neutrinos because they do not cause ionisation due to their weak interaction with matter. In the process of alpha decay the most of the decay energy (> 99%) is received by the alpha particle so the effect of the recoiling daughter nuclide was also omitted. The gamma emissions of ^{214}Pb and ^{214}Bi are incorporated in the external radiation measurement.

Measurements of external radiation

We measured external radiation with a scintillation gamma spectrometer system. NaI(Tl) detector (76 × 76 mm) was placed in a shelter made of a glass-fibre box and polyurethane foam as a thermal insulator. A constant temperature was maintained in the shelter to avoid the gain drift of the detector with a varying outdoor temperature. A computer add-on board (Oxford Instruments PCA-P) containing a high-voltage supply for the photomultiplier tube, a shaping amplifier and a 1024-channel pulse height analyser recorded the energy spectra of the ambient gamma radiation field. We obtained the energy spectra between 100 and 3000 keV in ten-minute intervals. A digital spectrum stabiliser that monitored the channel location of the ^{40}K gamma peak (1460 keV) kept the total gain of the system constant.

We converted the observed count rates to the dose rate units with a calibration factor obtained in a comparison to a pressurised ionisation chamber (Eberline FHT191N). This instrument was calibrated at STUK — Radiation and Nuclear Safety Authority. Owing to the high count rate of the scintillation detector system (200–400 s^{-1}) the one σ counting error was less than 1%. We calculated ion production rate from the dose rate values by assuming an average energy of 34 eV per produced ion pair and air density of 1.29 kg m^{-3}.

Accuracy of the ion production rate measurement

The uncertainty of the ion production rate results depends both on stochastic and systematic errors. As we mentioned above the stochastic counting error of the scintillation detector system is smaller than 1% and with the radon progeny from a few to several dozens of per cent. A systematic error of the external dose rate measurements might be created if the energy spectrum of the ambient gamma radiation field would be significantly distorted. However, during the observation period no exceptional airborne or deposited radioactivity was recorded in Finland (Mustonen 2006). The second systematic error is the use of constant density for the air when converting the dose rate to ion pair production.

For the ^{222}Rn activity concentration a source of a systematic error is the assumption that ^{222}Rn is in equilibrium with its short-lived daughter nuclides. In the case of turbulent conditions and long-range transported radon the disequilibrium can be expected to be small. However, the disequilibrium is more significant during surface inversions (Fontan *et al*. 1966). However, the air inlet is 6 m above ground which allows some time for the short-lived progeny to grow in after the exhalation of radon under such conditions. The second systematic error is the exclusion of any other airborne radionuclides except ^{222}Rn. However, in the most cases all the other airborne natural and artificial radionuclides exist in the air in such low activity concentrations that their influence on the ion production rate is negligible. In the air there are only a few μBq m^{-3} of artificial radionuclides, e.g. ^{137}Cs, a few hundred μBq m^{-3} of ^{210}Pb, a few mBq m^{-3} of ^{220}Rn progeny, a few mBq m^{-3} of ^{7}Be, a couple of hundred mBq m^{-3} of ^{14}C and minute amounts of other cosmogenic nuclides (Eisenbud 1987, Mattsson *et al*. 1996, Paatero and Hatakka 2000, Mustonen 2006). The only exception is ^{85}Kr, which originates mainly from the reprocessing plants of spent nuclear fuel, e.g. Sellafield, UK (Wilhelmova *et al*. 1995). Its activity concentration in the air is around 1 Bq m^{-3}. However, its contribution to the ion production rate is small as it emits only beta particles.

Measurements of ion mobility and size distributions

In order to study the effect of ion production rate on air ions, we measured air ion mobility distributions with a Balanced Scanning Mobility Analyzer (BSMA, manufactured by AIREL Ltd., Estonia). The ion mobility distribution measurements with the BSMA began in Hyytiälä in March 2003.

Tammet (2004, 2006) described the BSMA and its functioning in detail; here we give only a short review of the device. The BSMA measures the mobility distributions of small air ions and naturally charged nanometre particles in the range of 3.2–0.032 cm^2 V^{-1} s^{-1}. We calculated the corresponding diameter range (0.42–7.5 nm) for size distributions by utilising the algorithm described by Tammet (1995, 1998).

The BSMA consists of two identical plain type-differential mobility analysers; one analyser scans and measures positive ion mobility distributions, and the second negative ion distributions. The two mobility analysers and their common electrical amplifier are connected as a balanced bridge circuit. Inside each analyser there is one collecting element connected to common electrometer to measure the electrical current carried by the air ions.

Electro-filters, which are plates connected either to the ground or high voltage, at the inlets of the analysers form an inlet gate for the air ions and produce sheath air. The middle part of the inlet gate is electronically controlled: the gate is closed or opened for the ions. The inlet gate is opened when the BSMA measures sample air and closed when the BMSA verifies the offset level of the measuring electrometer. Measurement algorithm calculates the mobility distributions based on the sample air measurements and error in the distributions based on the offset level verifications.

The high air flow of the BSMA (22 l s^{-1} per analyser) enables to suppress the losses of the smallest air ions. The time resolution of the obtained size distributions was 15 minutes until the mid-August 2005, after which the time resolution was 10 minutes.

Results and discussions

We began ^{222}Rn measurements in March 2000 and external radiation measurements in October 2000. During the years we had several long breaks in the measurements. Therefore, we calculated various average characteristics based on our dataset to find out the long-term, seasonal and diurnal evolution of both the ^{222}Rn activity concentration and dose rate of external radiation. Based on these results we calculated ion production rate in order to get a long-term dataset to be used, for example, in aerosol particle formation research.

^{222}Rn activity concentration and external radiation dose rate

The average ^{222}Rn activity concentration in March 2000–June 2006 was 1.84 ± 1.35 Bq m^{-3} (median = 1.49 Bq m^{-3}) (Table 1). Blaauboer and Smetsers (1997) obtained similar results in the Netherlands. In Hyytiälä, the ^{222}Rn activity concentration varied between 0 and 11.1 Bq m^{-3}. The average external radiation dose rate for the whole measurement period was 0.13 ± 0.03 μGy h^{-1} (median = 0.14 μGy h^{-1}) (Table 1). The variation range was 0.06–0.23 μGy h^{-1}. These values are typical in Finland (Mattsson 1970, Observations of Radioactivity 1982, 1984, Mustonen 2006). This suggests that the results we obtained can be generalised across Finland as local peculiarities are not evident (Arvela 1995).

Table 1. The ^{222}Rn activity concentration and external radiation dose rate during March 2000–June 2006. The presented results were calculated from one hour average values.

	^{222}Rn activity concentration (Bq m^{-3})	External radiation dose rate (μGy h^{-1})
Min	0	0.06
10% value	0.48	0.08
25% value	0.85	0.11
Median	1.49	0.14
75% value	2.45	0.16
90% value	3.70	0.17
Max	11.1	0.23
Mean	1.84	0.13
SD	1.35	0.03

The activity concentration of ^{222}Rn demonstrated both the seasonal and diurnal variation, whereas the external radiation dose rate showed only a strong seasonal dependence with practically non-existing diurnal variation (Fig. 2). The distributions in Fig. 2 represent average activity concentrations and dose rates as the function of the hour of day and month. We utilised the whole dataset when calculating these averages.

We found the minimum ^{222}Rn activity concentrations in spring (Fig. 2), when the radon exhalation rate was at its minimum due to the wet snow cover, high ground-water level and frozen surface soil. Additionally, the vertical mixing of the boundary layer was efficient due to the long day light duration. In late summer and autumn, the diurnal variation was at its maximum due to the simultaneous strong radon exhalation, caused by the drying and warming surface soil and low ground-water level (Mattsson 1970, Stranden *et al.* 1984), and frequent nocturnal surface inversions. In winter, the diurnal variation was almost non-existing and the activity concentration was close to its maximum due to the stable conditions in the troposphere owing to the lack of solar radiation. The concentrations decreased towards the spring because the thickening snow cover gradually decreased the radon exhalation rate.

Our results of the external radiation dose rate showed a strong seasonal variation (Fig. 2). The flux of gamma radiation (one of the two main external radiation components) from the ground is controlled by the water content of the surface soil and the water content of the snow cover. Therefore, the external radiation dose rate was at its maximum in late summer and autumn when the surface soil was dry. The minimum occurred in late winter and spring when the water content of the snow cover was at its maximum. The other main external radiation component, cosmic radiation has only a minimal seasonal cycle, which is caused by the changes in the vertical pressure profile of the atmosphere (Tanskanen 1965). This cycle was, however, hidden by the variations of gamma radiation from the ground. Earlier, Hatakka *et al.* (1998) studied the correlation between radon activity concentration and dose rate at Tikkakoski, 100 km north-east of Hyytiälä, during the maximum diurnal varia-

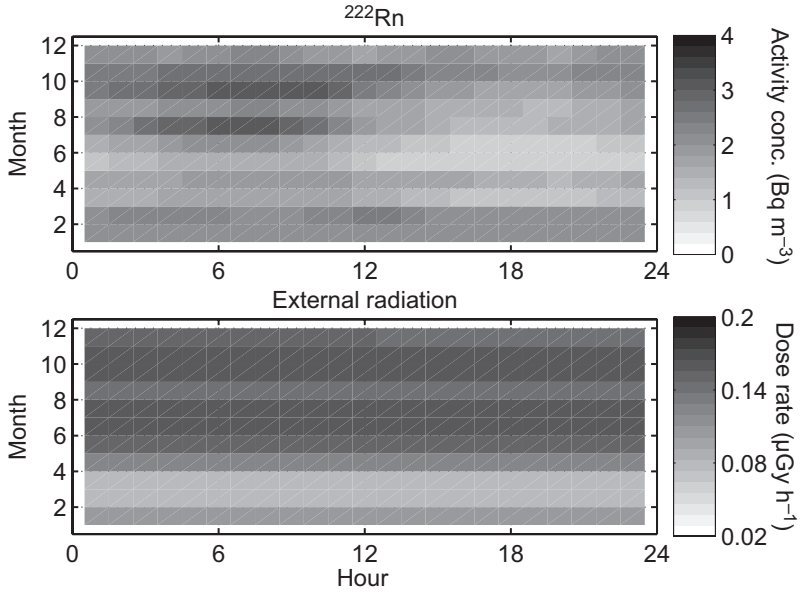

Fig. 2. The average activity concentration of ^{222}Rn and dose rate of external radiation as the function of the hour of day (UTC + 2) and month based on measurements between March 2000 and June 2006. The radon activity concentrations were additionally averaged with four hour time window.

tion of radon activity concentration in July–September. They found that even though the radon activity concentration was more than doubled from afternoon to early morning the dose rate increased only 0.5%.

When studying the wind direction dependence of the ^{222}Rn activity concentrations (Fig. 3), we considered only the data starting on 5 Sep. 2003, since our wind direction measurements at 8.4 m height (inside the canopy) were initiated then with an ultrasonic anemometer (Ultrasonic anemometer 2D, Adolf Thies GmbH, Göttingen, Germany). Only the winds faster than 1 m s^{-1} were included in this analysis to ensure the mixing of the air also inside the canopy. We observed the highest ^{222}Rn activity concentrations when the wind was from south-east (Fig. 3). Radon has accumulated to the air masses coming to Finland from continental regions (Baskaran *et al.* 1993). Furthermore, we observed the lowest ^{222}Rn activity concentrations during the winds from north-west. Maritime air masses coming from the North Atlantic Ocean have low ^{222}Rn-content because the oceans are the negligible sources of radon. When the wind speed was below 1 m s^{-1} the average ^{222}Rn concentration was 1.9 Bq m^{-3} and median was 1.6 Bq m^{-3}.

The difference between early morning and afternoon ^{222}Rn activity concentrations can be considered a rough estimate of the local radon sources. From the results (Fig. 3) one can deduce that local sources are quite uniformly distributed around the monitoring station because the difference does not show any particular wind direction dependence.

Ion production rate

Variation range of ion production rate

Ion production rate by ^{222}Rn varied in the range 0–6.5 ion pairs cm^{-3} s^{-1}, with average and median values 1.1 and 0.9 ion pairs cm^{-3} s^{-1}, respectively (Fig. 4 and Table 2). Ion production by external radiation varied in the range 4.0–15.3 ion pairs cm^{-3} s^{-1}. The average and median values were 8.7 and 9.5 ion pairs cm^{-3} s^{-1}. The corresponding values for the total ion production rate were: the variation range was 4.2–17.6 ion pairs cm^{-3} s^{-1} with the average and median of 10.1 and 10.4 ion pairs cm^{-3} s^{-1}, respectively. The total ion production was dominated by the effect of external radiation (Table 2). During our measurement period the contribution of external radiation ranged from 57% to 100%. On average the contribution of the external radiation was 89% (median 91%). We have to note that the total ion production rate represents only the periods when we had the data for both the ^{222}Rn and external

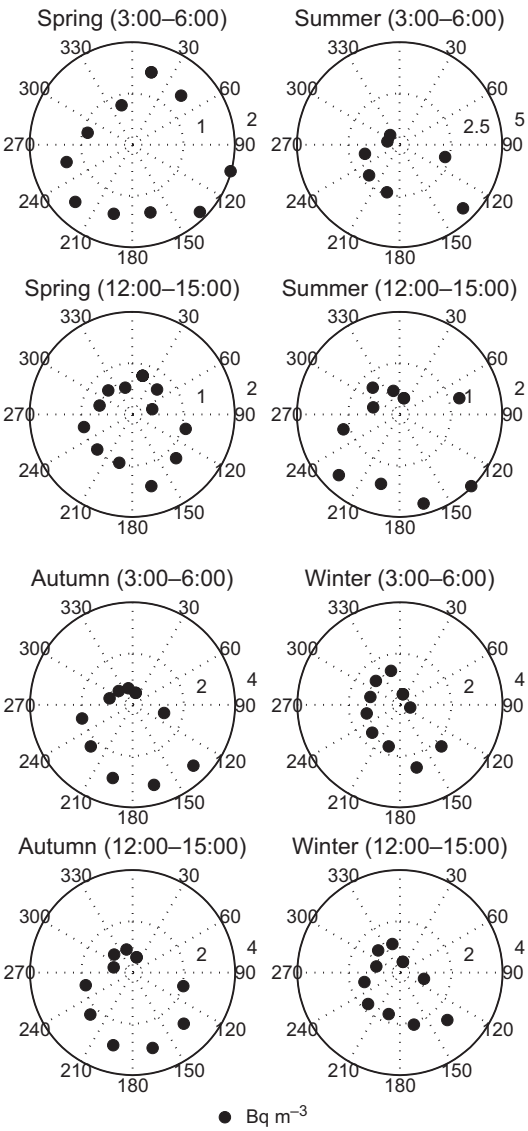

Fig. 3. The average ^{222}Rn activity concentrations as a function of wind direction for spring, summer, autumn and winter. The results are shown for periods between 3:00–6:00 and 12:00–15:00 (UTC + 2). Only the concentrations, when wind speed was higher than 1 m s^{-1} inside the canopy, were considered when calculating the presented average values.

radiation. Fortunately, we have the information on the total ion production rate continuously for over a year on two occasions between March 2000 and June 2006.

Laakso *et al*. (2004) calculated the ion production rate based on the ion and particle size distribution measurements and balance equation for cluster (typically smaller than 1.8 nm in diameter) ions (Israël 1970). They investigated ion production in Hyytiälä in spring 2003 for one month; this period is included in our dataset. They obtained smaller values based on calculations (on average 2.6 ion pairs cm^{-3} s^{-1} at 2-m height) than via the direct measurements (on average 4.5 ion pairs cm^{-3} s^{-1} at the 6 m height). There has to be some additional sink for ions, which Laakso *et al*. (2004) could not include in their study.

Tammet *et al*. (2006) also calculated ion production rate based on the ion and particle size distribution measurements in Hyytiälä in August 2005 and balance equation. In addition to cluster ion recombination and attachment to larger particles, Tammet *et al*. (2006) considered the dry deposition of these small ions onto tree surfaces (needles and leaves). Based on their short measurement period in Hyytiälä, Tammet *et al*. (2006) obtained ion production rates on average 5.6 ± 0.8 and 3.9 ± 0.2 ion pairs cm^{-3} s^{-1} at 2 and 14 m, respectively. At the same time, based on our radiation measurements, we obtained the total ion production rate values between 10.9 and 12.2 ion pairs cm^{-3} s^{-1} at 6 m height. The period, which Tammet *et al*. (2006) studied, was night time and no particle formation, rain or other phenomenon that could modify the size distributions or radiation measurement results in unexpected way occurred. This means that there is still some discrepancy between straight radiation measurements and theoretical approach. We have to also consider the accuracy of measuring instrumentation, which certainly makes some discrepancy in the results.

Temporary ion production rate depends on many parameters like the content of radioactive substances and water in soil, snow cover, the nature of terrain and the mixing state of boundary layer. For comparison with the results from Hyytiälä, Dhahorkar and Kamra (1994) observed high variability in ion production rate (2.65–116.52 ion pairs cm^{-3} s^{-1}) during their four day measurement period in Pune, India. They observed the lowest values in the afternoon, when the mixing of the boundary layer was highest, and the highest values in the early morning. Vartiainen *et al*. (2007) observed high variation in ion production (0.1–30 ion pairs cm^{-3} s^{-1}) due

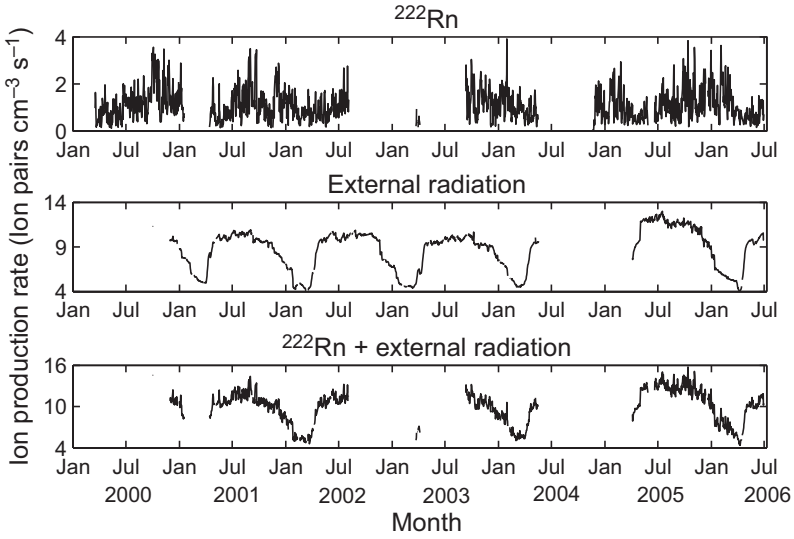

Fig. 4. Ion production rate as a function of month by ^{222}Rn, external radiation, and the sum of ^{222}Rn and external radiation.

to radon decay during their two weeks train trip through Siberia. They did not measure external radiation or its components.

Seasonal and diurnal variation of the ion production rate

Ion production by ^{222}Rn did not vary significantly from year to year, but more clearly in a seasonal scale. Ion production by ^{222}Rn could reach its highest values in summer, autumn or winter but never in spring when the ground was wet due to snow and water (Fig. 4). In spring, summer and autumn ion production by ^{222}Rn had diurnal patterns with maximum during morning hours and minimum during evening (Fig. 5). These observations were due to the vertical mixing behaviour of boundary layer. In winter, the diurnal variation was less pronounced. The ion production rate by external radiation did not show any diurnal variation but clear seasonal dependence with the highest values in summer and autumn (Figs. 4 and 5). In 2005, the ion production by external radiation reached slightly higher values than during the other years (Fig. 4). The total ion production was mostly due to the external radiation (Figs. 4 and 5).

We measured also the air ion size distributions with a balanced scanning mobility ana-

Table 2. The ion production rate by ^{222}Rn, external radiation and total (^{222}Rn + external radiation), and the ratio of the ion production rate by ^{222}Rn to ion production by external radiation and the total ion production rate during March 2000–June 2006. The presented results were calculated from one hour average values.

	^{222}Rn (ion pairs cm^{-3} s^{-1})	External radiation (ion pairs cm^{-3} s^{-1})	Total (ion pairs cm^{-3} s^{-1})	Ratio of ion production by ^{222}Rn to external radiation	Ratio of ion production by ^{222}Rn to total ion production
Min	0	4.0	4.2	0	0
10%	0.3	5.0	6.1	0.03	0.03
25%	0.5	6.9	8.8	0.06	0.05
Median	0.9	9.5	10.4	0.10	0.09
75%	1.4	10.3	11.7	0.17	0.15
90%	2.2	11.4	12.9	0.26	0.20
Max	6.5	15.3	17.6	0.75	0.43
Mean	1.1	8.7	10.1	0.13	0.11
SD	0.8	2.3	2.4	0.10	0.07

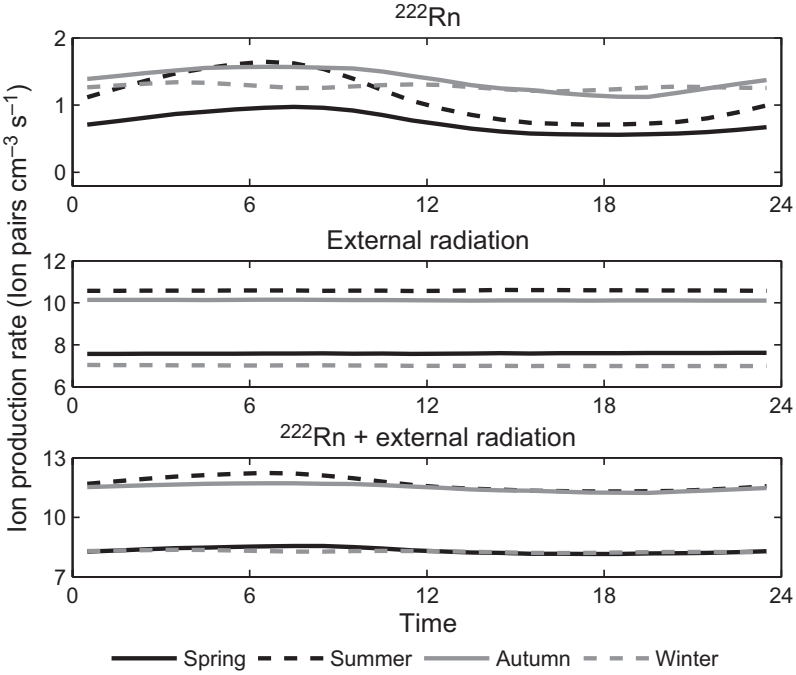

Fig. 5. Seasonal ion production rate by ^{222}Rn, external radiation, and the sum of ^{222}Rn ,and external radiation. The radon activity concentrations were additionally averaged with four-hour time window (UTC + 2).

lyzer in Hyytiälä. We utilised the period between March 2003 and June 2006 when comparing cluster ion (smaller than 1.8 nm in diameter) concentrations and the total ion production rate (Fig. 6). Based on our results we did not observe strong correlation between these two parameters. Although, the highest cluster concentrations were observed only when the ion production rate was higher than approximately 9 ion pairs cm^{-3} s^{-1}.

However, we obtained a strong dependence of the cluster ion concentrations to the total ion production rate divided by condensation sink (CS) (Fig. 7). The CS (s^{-1}) describes the loss rate of air molecules to the pre-existing aerosol

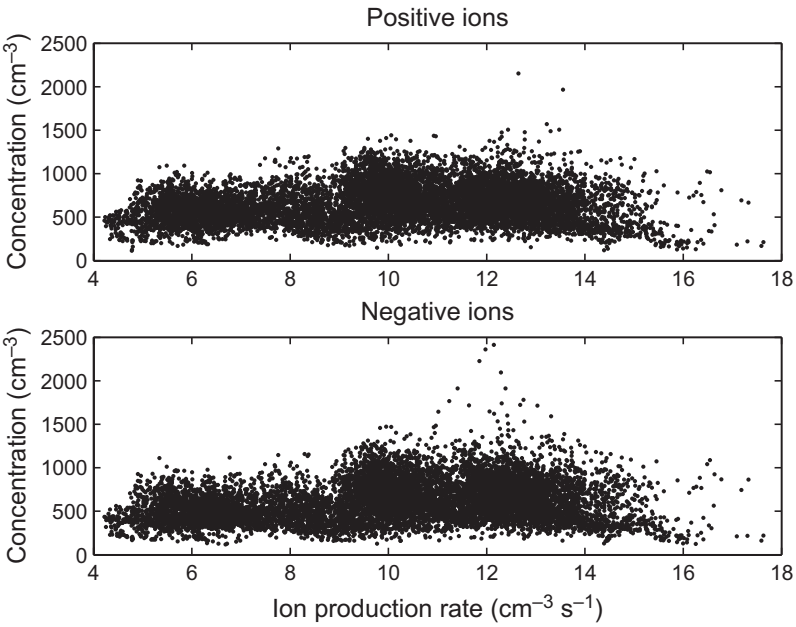

Fig. 6. Concentrations of cluster ions (smaller than 1.8 nm in diameter) as a function of total ion production rate. The presented results are one-hour average values.

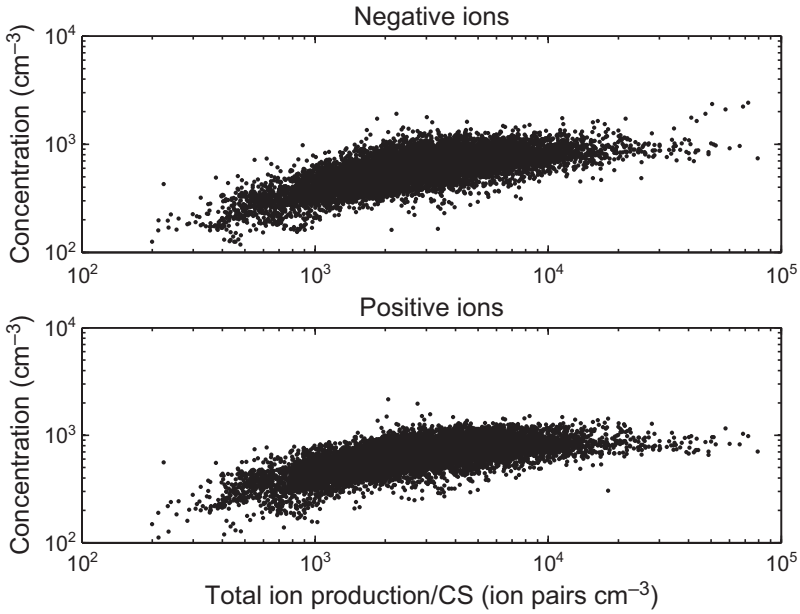

Fig. 7. Concentrations of cluster ions (smaller than 1.8 nm in diameter) as a function of total ion production rate divided by condensation sink (CS). The presented results are one-hour average values.

particles. We calculated the CS from particle size distributions as described for example by Pirjola *et al*. (1999), Kulmala *et al*. (2001a) and Dal Maso *et al*. (2005). We also took into account the particle hygroscopic growth, which was parameterised based on the measurements in Hyytiälä (Hämeri *et al*. 2001, Laakso *et al*. 2004).

When the ratio of the total ion production rate to CS was at its lowest we observed smallest cluster ion concentrations, and their concentration increased when the ratio increased. The correlation coefficient between the cluster ion concentration and ion production to CS ratio was 0.43 and 0.52 for positive and negative clusters, respectively. Our results indicate that cluster ion sink due to their attachment on pre-existing aerosol particles had a strong influence on their concentrations in Hyytiälä. Also other sinks like recombination, deposition on tree surfaces and particle formation via both the neutral and ion-induced mechanisms are known to have effect on cluster ion concentrations (Israël 1970, Tammet *et al*. 2006). In contrast to our results, Vartiainen *et al*. (2007) observed good correlation between cluster ion concentrations and ion production due to radon decay during their train trip through Siberia. Based on their results the ion production had more effect on cluster ion concentration than the coagulation loss or attachment on pre-existing aerosol particles.

Ion production and secondary particle formation

Do some particle formation characteristics depend on the ion production rate? Such characteristics could for example be the frequency of secondary particle formation events, concentration of charged particles during particle formation and growth rate of small particles. Dal Maso *et al*. (2005) observed the highest number of particle formation events in Hyytiälä in spring (March–May) and autumn (September). The formation event frequency of charged aerosol particles followed that observed with the whole aerosol population (Hirsikko *et al*. 2006). Based on our results of the ion production rate we cannot draw any certain conclusions whether the ion production has an effect on the frequency of particle formation or not. However, it is known that the concentrations of nucleating and condensing vapours, and different vapour and particle sink terms affect significantly on particle formation process (e.g. Kulmala *et al*. 2001a, Kulmala *et al*. 2004a, Kulmala *et al*. 2006).

The concentration of charged particles during the particle formation depends on nucleation mechanism (i.e. ion-induced *versus* neutral nucleation), nucleation rate and the charging probability of the particles. The contribution of ion induced nucleation can be evaluated with

some new aerosol instruments (*see* Laakso *et al*. 2007) or by combining model calculations and observations about ion size distributions. The contribution of the ion-induced nucleation varies form day to day (Laakso *et al*. 2007). However, lacking information about nucleation mechanisms of each particle formation events during our measurement period prevents us to directly compare the importance of ion production rate to ion-induced nucleation or its rate.

It is known that electric charge on particles enhance the growth of smallest particles, especially smaller than 3 nm in diameter (e.g. Yu and Turco 2000, Laakso *et al*. 2003). As discussed by Kulmala *et al*. (2004b) the growth is enhanced by electric charge (i.e. the indication of the ion-induced nucleation) if the growth rate of particles decrease as a function of size. In summer, the growth of different sized particles (larger than 3 nm in diameter) was faster than the growth of the smallest particles (smaller than 3 nm in diameter) in Hyytiälä (Hirsikko *et al*. 2005). While in winter, the growth rate decreased or was stable as a function of particle diameter indicating the importance of the electric charge on the growth of the smallest particles (Hirsikko *et al*. 2005). Although during winter the total ion production rate was still quite high, it decreased towards the spring and obtained maximum value in summer and autumn. Thus this kind of comparison based on statistical growth rates can cause misleading conclusions. The concentrations of condensing vapours (like H_2SO_4 and organics) affect substantially the particle growth. For example the organic vapour concentrations are highest in summer (Hakola *et al*. 2003), which correlates with the faster growth of larger particles. To draw more detailed conclusions on the effect of ion production rate on particle growth we should study the correlation between the ion production, particle formation mechanism, growth rate of particles, and condensing vapour concentrations during each individual particle formation.

Summary

We measured the ^{222}Rn content of air and external radiation at Hyytiälä forest station in Finland during March 2000–June 2006. Here we presented daily, seasonal and long-term variations of the ^{222}Rn activity concentration and external radiation dose rate based on six years and three months dataset. We observed the ^{222}Rn activity concentration to vary in the range 0–11.1 Bq m^{-3} and the external radiation dose rate in the range 0.06–0.23 μGy h^{-1}. The annual cycle of these parameters were similar from year to year and their seasonal variations were clear. Only the ^{222}Rn activity concentration had season dependent diurnal cycle with the highest values in the morning.

We calculated ion production rate based on ^{222}Rn and external radiation measurements in the lower boundary layer. Here, we presented so far the longest dataset for the ion production in a Finnish boreal forest. Our results are valuable for all who study the ion-induced nucleation, which is limited by the ion production. According to our measurements, we cannot observe larger ion-induced nucleation rates than 17.6 cm^{-3} s^{-1} in Hyytiälä. We found that external radiation contributed the most on the total ion production rate; on average the external radiation contribution was 89%. During the whole measurement period the ion production rates by ^{222}Rn, external radiation and the total were on average 1.1, 8.7 and 10.1 ion pairs cm^{-3} s^{-1}, respectively. The detailed analysis of the significance of ion production rate on particle formation frequency, charged particle concentration during particle formation and particle growth rates requires further information than was available during this study.

Acknowledgements: Anne Hirsikko acknowledges Maj and Tor Nessling foundation (grant nr 2006168) for the financial support. The authors thank Mr. Veijo Hiltunen for the routine maintenance of the instruments at Hyytiälä and Miikka Dal Maso from the University of Helsinki for providing information.

References

Arvela H. 1995. *Residential radon in Finland: sources, variation, modelling and dose comparisons*. STUK-A124, STUK — Radiation and Nuclear Safety Authority, Helsinki.

Baskaran M., Coleman C.H. & Santschi P.H. 1993. Atmospheric depositional fluxes of ^{7}Be and ^{210}Pb at Galveston and College Station, Texas. *J. Geophys. Res*. 98: 20555–20571.

Blaauboer R.O. & Smetsers R.C.G.M. 1997. Outdoor concentrations of the equilibrium-equivalent decay products of ^{222}Rn in the Netherlands and the effect of meteorological variables. *Radiat. Prot. Dosim.* 69: 17–18.

Dal Maso M., Kulmala M., Riipinen I., Wagner R., Hussein T., Aalto P.P. & Lehtinen K.E.J. 2005. Formation and growth of fresh atmospheric aerosols: eight years of aerosol size distribution data from SMEAR II, Hyytiälä, Finland. *Boreal Env. Res.* 10: 323–336.

Dhanorkar S. & Kamra A.K. 1994. Diurnal variation of ionization rate close to ground. *J. Geophys. Res.* 99: 18523–18526.

Eisenbud M. 1987. *Environmental radioactivity from natural, industrial, and military sources.* Academic Press, Inc., Orlando, USA.

Fontan J., Birot A., Blanc D., Bouville A. & Druilhet A. 1966. Measurement of the diffusion of radon, thoron and their radioactive daughter products in the lower layers of the Earth's atmosphere. *Tellus* 18: 623–632.

Gesell T.F. 1983. Background atmospheric ^{222}Rn concentrations outdoors and indoors: a review. *Health Phys.* 45: 289–302.

Hakola H., Tarvainen V., Laurila T., Hiltunen V., Hellén H. & Keronen P. 2003. Seasonal variation of VOC concentrations above a boreal coniferous forest. *Atmos. Environ.* 37: 1623–1634.

Hari P. & Kulmala M. 2005. Station for Measuring Ecosystem–Atmosphere Relations (SMEAR II). *Boreal Env. Res.* 10: 315–322.

Hatakka J., Paatero J., Viisanen Y. & Mattsson R. 1998. Variations of external radiation due to meteorological and hydrological factors in central Finland. *Radiochemistry* 40: 534–538.

Hirsikko A., Laakso L., Hõrrak U., Aalto P.P., Kerminen V.-M. & Kulmala M. 2005. Annual and size dependent variation of growth rates and ion concentrations in boreal forest. *Boreal Env. Res.* 10: 357–369.

Hirsikko A., Bergman T., Laakso L., Dal Maso M., Riipinen I., Hõrrak U. & Kulmala M. 2006. Identification and classification of the formation of intermediate ions measured in boreal forest. *Atmos. Chem. Phys. Discuss.* 6: 9187–9212.

Hõrrak U., Salm J. & Tammet H. 2003. Diurnal variation in the concentration of air ions of different mobility classes in a rural area. *J. Geophys. Res.* 108(D20), 4653, doi:10.1029/2002JD003240.

Hämeri K., Väkevä M., Aalto P.P., Kulmala M., Swietlicki E., Zhou J., Seidl W., Becker E. & O'Dowd C.D. 2001. Hygroscopic and CCN properties of aerosol particles in boreal forests. *Tellus* 53B: 359–379.

Israël H. 1970. *Atmospheric electricity, vol. 1: Fundamentals, conductivity, ions.* Israel Program for Scientific Translations, Jerusalem.

Kulmala M., Dal Maso M., Mäkelä J.M., Pirjola L., Väkevä M., Aalto P., Miikkulainen P., Hämeri K. & O'Dowd C.D. 2001a. On the formation, growth and composition of nucleation mode particles. *Tellus* 53B: 479–490.

Kulmala M., Hämeri K., Aalto P.P., Mäkelä J.M., Pirjola L., Nilsson E.D., Buzorius G., Rannik Ü., Dal Maso M., Seidl W., Hoffman T., Janson R., Hansson H.-C., Viisanen Y., Laaksonen A. & O'Dowd C.D. 2001b. Overview of the international project on biogenic aerosol formation in the boreal forest (BIOFOR). *Tellus* 53B: 324–343.

Kulmala M. 2003. How particles nucleate and grow. *Science* 302: 1000–1001.

Kulmala M., Vehkamäki H., Petäjä T., Dal Maso M., Lauri A., Kerminen V.-M., Birmili W. & McMurry P.H. 2004a. Formation and growth rates of ultrafine atmospheric particles: A review of observations. *J. Aerosol Sci.* 35: 143–176.

Kulmala M., Laakso L., Lehtinen K.E.J., Riipinen I., Dal Maso M., Anttila T., Kerminen V.-M., Hõrrak U., Vana M. & Tammet H. 2004b. Initial steps of aerosol growth. *Atmos. Chem. Phys.* 4: 2553–2560.

Kulmala M., Lehtinen K. E. J. & Laaksonen A. 2006. Cluster activation theory as an explanation of the linear dependence between formation rate of 3 nm particles and sulphuric acid concentration. *Atmos. Chem. Phys.* 6: 787–793.

Laakso L., Kulmala M. & Lehtinen K.E.J. 2003. Effect of condensation rate enhancement factor on 3-nm (diameter) particle formation in binary ion-induced and homogeneous nucleation. *J. Geophys. Res.* 108(D18), 4574, doi:10.1029/2003JD003432.

Laakso L., Petäjä T., Lehtinen K.E.J., Kulmala M., Paatero J., Hõrrak U., Tammet H. & Joutsensaari J. 2004. Ion production rate in a boreal forest based on ion, particle and radiation measurements. *Atmos. Chem. Phys.* 4: 1933–1943.

Laakso L., Gagné S., Petäjä T., Hirsikko A., Aalto P., Kulmala M. & Kerminen V.-M. 2007. Detecting charging state of ultra-fine particles: instrumental development and ambient measurements. *Atmos. Chem. Phys.* 7: 1333–1345.

Mattsson R. 1970. Seasonal variation of short-lived radon progeny, Pb^{210} and Po^{210} in ground level air in Finland. *J. Geophys. Res.* 75: 1741–1744.

Mattsson R., Paatero J. & Hatakka J. 1996. Automatic alpha/beta analyser for air filter samples — absolute determination of radon progeny by pseudo-coincidence techniques. *Radiat. Prot. Dosim.* 63: 133–139.

Mustonen R. (ed.) 2006. *Surveillance of environmental radiation in Finland. Annual report 2005.* STUK-B-TKO 7. STUK — Radiation and Nuclear Safety Authority, Helsinki.

Observations of Radioactivity 1982, 1984. *Observations of radioactivity* no. 22. Finnish Meteorological Institute, Helsinki.

Paatero J. & Hatakka J. 2000. Source areas of airborne ^{7}Be and ^{210}Pb measured in northern Finland. *Health Phys.* 79: 691–696.

Paatero J., Hatakka J., Mattsson R. & Lehtinen I. 1994. A comprehensive station for monitoring atmospheric radioactivity. *Radiat. Prot. Dosim.* 54: 33–39.

Pirjola L., Kulmala M., Wilck M., Bischoff A., Stratmann F. & Otto E. 1999. Formation of sulphuric acid aerosols and cloud condensation nuclei: an expression for significant nucleation and model comparison. *J. Aerosol Sci.* 30: 1079–1094.

Porstendörfer J. 1994. Properties and behaviour of radon and thoron and their decay products in the air. *J. Aerosol Sci.* 25: 219–263.

Porstendörfer J. & Reineking A. 1999. Radon: characteristics in air and dose conversion factors. *Health Phys.* 76: 300–305.

Stranden E., Kolstad A.K. & Lind B. 1984. The influence of moisture and temperature on radon exhalation. *Radiat. Prot. Dosim.* 7: 55–58.

Tammet H. 1995. Size and mobility of nanometer particles, clusters and ions. *J. Aerosol Sci.* 26: 459–475.

Tammet H. 1998. Reduction of air ion mobility to standard conditions. *J. Geophys. Res.* 103: 13 933–13 937.

Tammet H. 2004. Balanced scanning mobility analyzer, BSMA. In: Kasahara M. & Kulmala M. (eds.), *Nucleation and atmospheric aerosols 2004, 16th International Conference*, Kyoto University Press, Japan, pp. 294–297.

Tammet H. 2006. Continuous scanning of the mobility and size distribution of charged clusters and nanometer particles in atmospheric air and the Balanced Scanning Mobility Analyzer BSMA. *Atmos. Res.* 82: 523–535.

Tammet H., Hõrrak U., Laakso L. & Kulmala M. 2006. Factors of ion balance in coniferous forest according to measurements in Hyytiälä, Finland. *Atmos. Chem. Phys.* 6: 3377–3390.

Tanskanen P.J. 1965. On the variation of cosmic ray meson intensity at sea level in connection with atmospheric disturbances. *Ann. Acad. Sci. Fenn.* AVI 185: 1–96.

Vartiainen E., Kulmala M., Ehn M., Hirsikko A., Junninen H., Petäjä T., Sogacheva L., Kuokka S., Hillamo R., Skorokhod A., Belikov I., Elansky N. & Kerminen V.-M. 2007. Ion and particle number concentrations and size distributions along the Trans-Siberian railroad. *Boreal Env. Res.* 12: 375–396.

Wilhelmova L., Tomasek M. & Stukheil K. 1995. Monitoring of krypton-85 activity in the atmosphere around Prague. *Environ. Monit. Assess.* 34: 145–149.

Yu F. & Turco R.P. 2000. Ultrafine aerosol formation via ion-mediated nucleation. *Geophys. Res. Lett.* 27: 883–886.